REPORT No. 800

EFFECTS OF SMALL ANGLES OF SWEEP AND MODERATE AMOUNTS OF DIHEDRAL ON STALLING AND LATERAL CHARACTERISTICS OF A WING-FUSELAGE COMBINATION EQUIPPED WITH PARTIAL- AND FULL-SPAN DOUBLE SLOTTED FLAPS

By JEROME TEPLITZ

SUMMARY

Tests of a wing-fuselage combination incorporating NACA 65-series airfoil sections were conducted in the NACA 19-foot pressure tunnel. The investigation included tests with flaps neutral and with partial- and full-span double slotted flaps deflected to determine the effects of (1) variations of wing sweep between −4° and 8° on stalling and lateral stability and control characteristics and (2) variations of dihedral between 0° and 6.75° on lateral stability characteristics.

Deflection of the flaps noticeably reduced dihedral effect. Sweepback increased considerably the effective dihedral and decreased the adverse effect of flap deflection on dihedral effect; sweepforward reduced the effective dihedral and increased the adverse effect of flap deflection. More favorable variations of effective dihedral with lift coefficient were obtained with sweepback.

Stalling characteristics were less satisfactory with sweepback than with normal sweep or sweepforward in that the point of initial stall moved outboard, but increased maximum lift coefficients were noted for every flap condition. Aileron effectiveness was reduced about 10 percent with sweepback and flaps neutral but varied little with sweep with the flaps deflected.

Agreement with theory was noted for the effect of changes in dihedral angle on lateral stability characteristics. The test results showed that the change in slope of the curve of rolling-moment coefficient against angle of yaw was approximately 0.00026 per degree change in geometric dihedral angle.

INTRODUCTION

Many of the effects of sweep and dihedral on lateral stability have been determined in previous theoretical and experimental investigations. (See, for example, references 1 and 2.) However, the applicability of these results to airplanes having wings of low-drag sections and/or equipped with such high-lift devices as double slotted flaps is uncertain.

In order to provide information relative to this problem, tests were conducted in the NACA 19-foot pressure tunnel on a wing-fuselage combination provided with partial- and full-span double slotted flaps and incorporating NACA 65-series airfoil sections. The investigation, conducted at a Reynolds number of approximately 3×10^6, included stalling and lateral-stability and control tests covering a range of sweep angle from −4° to 8° and a range of dihedral angle from 0° to 6.75° with flaps neutral and deflected.

MODEL AND APPARATUS

The model used for the present tests was the bare wing and fuselage of a 0.2375-scale model of an attack-bomber airplane. The wing of the model for the normal-sweep condition is of NACA 65(216)–215, $a=0.8$ section at the root and NACA 65(216)–215, $a=0.5$ section at the tip. The root incidence is 2° with respect to the fuselage reference line and the tip incidence is 1°. The geometric washout is 1° and the corresponding aerodynamic washout is approximately 1.3°. The aspect ratio is 9.08 and the taper ratio is 2.21. No wing-fuselage fillets were used for these tests. General views and principal dimensions of the model are given in figure 1.

The wing sweep was changed by rotating each panel about an axis on the 20-percent chord line and 5.4 percent of the semispan outboard of the plane of symmetry. At the normal dihedral angle of 4.5°, three sweep settings were tested: normal sweep (20-percent chord line straight), sweepforward (−10-percent chord line straight), and sweepback (110-percent chord line straight). The sweep of the 25-percent chord line for the three conditions was approximately −1°, −4°, and 8°, respectively.

The dihedral setting of the wing was changed by rotating each panel about an axis located on the 20-percent chord line and 7.6 percent of the semispan outboard of the plane of symmetry. Three dihedral settings, 4.5° (normal dihedral), 0°, and 6.75°, were tested at the normal sweep. All mechanism to change the wing sweep and dihedral angle was housed within the wing and fuselage.

The model was equipped with double slotted flaps extending from the fuselage to 65 percent of each semispan. The deflection was 55° for all runs with the flaps deflected. Flap details are given in figure 2.

The full-span-flap installation consisted of the double slotted partial-span flaps and "flaperons" or flap-ailerons. Flaperon details are given in figure 3. In the configurations with flaps retracted and partial-span flaps deflected, the aileron is of the simple slotted type. For the configuration with full-span flaps deflected, the aileron hinge point was moved rearward and down, the ailerons were drooped 25°, and vanes were installed ahead of the ailerons. For the ailerons-deflected tests, the ailerons were deflected differentially from the neutral positions of 0° and 25°, right aileron up 12° and left aileron down 9.3°. The vanes

remained fixed in relation to the wing when the drooped ailerons were deflected. The deflections correspond to approximately 60 percent of full deflection of the sealed ailerons used on the airplane.

The investigation was carried out in the NACA 19-foot pressure tunnel with the air in the tunnel compressed to an absolute pressure of 35 pounds per square inch. The model was mounted on the single-strut support system (fig. 4), which for these tests permitted an angle-of-attack range from −9° to 16° and an angle-of-yaw range from −30° to 30°. Force and moment characteristics were measured by a six-component, electrically recording balance system. Rolling moments were also measured by a resistance-type wire strain gage mounted on the support strut. Rolling moments measured by the strain gage have been presented in preference to those measured by the balance system.

TESTS

The wing-fuselage combination was tested with the flaps neutral and partial- and full-span flaps deflected at each of the three sweeps—normal, forward, and back. These tests were made with the wing dihedral in the normal position, 4.5°. Each configuration was tested at zero yaw with the ailerons neutral and differentially deflected through the available angle-of-attack range. At several constant angles of attack, yaw tests were made through a range of angle of yaw from −6° to 28°. In addition, stall studies were made for each configuration. The action of wool tufts attached to the upper surface of the wing and flaps was recorded by means of sketches, photographs, and motion pictures.

With the wing sweep in the normal position, the model was tested with the flaps neutral and partial- and full-span flaps deflected at dihedral angles of 0° and 6.75°. Each configuration was tested at zero yaw with ailerons neutral through the available angle-of-attack range and an angle-of-yaw range from −6° to 28° at the same constant angles of attack used in the sweep tests.

For each of the several flap deflections, therefore, pitch and yaw tests were made to give comparable results for three sweep conditions at the normal dihedral setting and for three dihedral settings at the normal sweep.

Because of structural limitations of the model and support system, the tunnel airspeed was changed with flap deflection. The test dynamic pressures and corresponding Reynolds and Mach numbers are as follows:

Model configuration		Dynamic pressure (lb/sq ft)	Reynolds number (approx.)	Mach number (approx.)
Flap deflection (deg)	Aileron droop (deg)			
0	0	50	3.6×10^6	0.12
55	0	35	3.1	.10
55	25	30	2.8	.09

The changes in Reynolds and Mach numbers are believed to be sufficiently small that the results may be compared directly.

COEFFICIENTS AND SYMBOLS

The coefficients and symbols are defined as follows:

C_L	lift coefficient $\left(\frac{\text{Lift}}{qS}\right)$
C_D	drag coefficient (D/qS)
C_Y	lateral-force coefficient (Y/qS)
C_m	pitching-moment coefficient $(M/qS\bar{c})$
C_n	yawing-moment coefficient (N/qSb)
C_l	rolling-moment coefficient (L/qSb)
α	angle of attack with respect to fuselage reference line, degrees
ψ	angle of yaw, degrees
Γ	dihedral angle, degrees
C_{l_ψ}	slope of curve of rolling-moment coefficient against angle of yaw $(\partial C_l/\partial\psi)$
C_{n_ψ}	slope of curve of yawing-moment coefficient against angle of yaw $(\partial C_n/\partial\psi)$
C_{Y_ψ}	slope of curve of lateral-force coefficient against angle of yaw $(\partial C_Y/\partial\psi)$
δ	control deflection, degrees
R	Reynolds number
M	Mach number
where	
q	dynamic pressure, pounds per square foot
b	wing span, feet
S	wing area, square feet (normal sweep, 30.488 sq ft; sweepforward, 30.611 sq ft; sweepback, 29.722 sq ft)
c	mean aerodynamic chord (1.920 ft)
D	drag
Y	lateral force
M	pitching moment
N	yawing moment
L	rolling moment
Subscripts	
a	aileron
f_{65}	65-percent-span double slotted flaps
r	right
l	left
max	maximum

RESULTS AND DISCUSSION

All data are referred to the stability axes, of which the Z-axis is in the plane of symmetry and perpendicular to the relative wind, the X-axis is in the plane of symmetry and perpendicular to the Z-axis, and the Y-axis is perpendicular to the plane of symmetry.

Moments were computed about center-of-gravity locations 25 percent behind the leading edge of the mean aerodynamic chord and 5.3 percent of the mean aerodynamic chord above

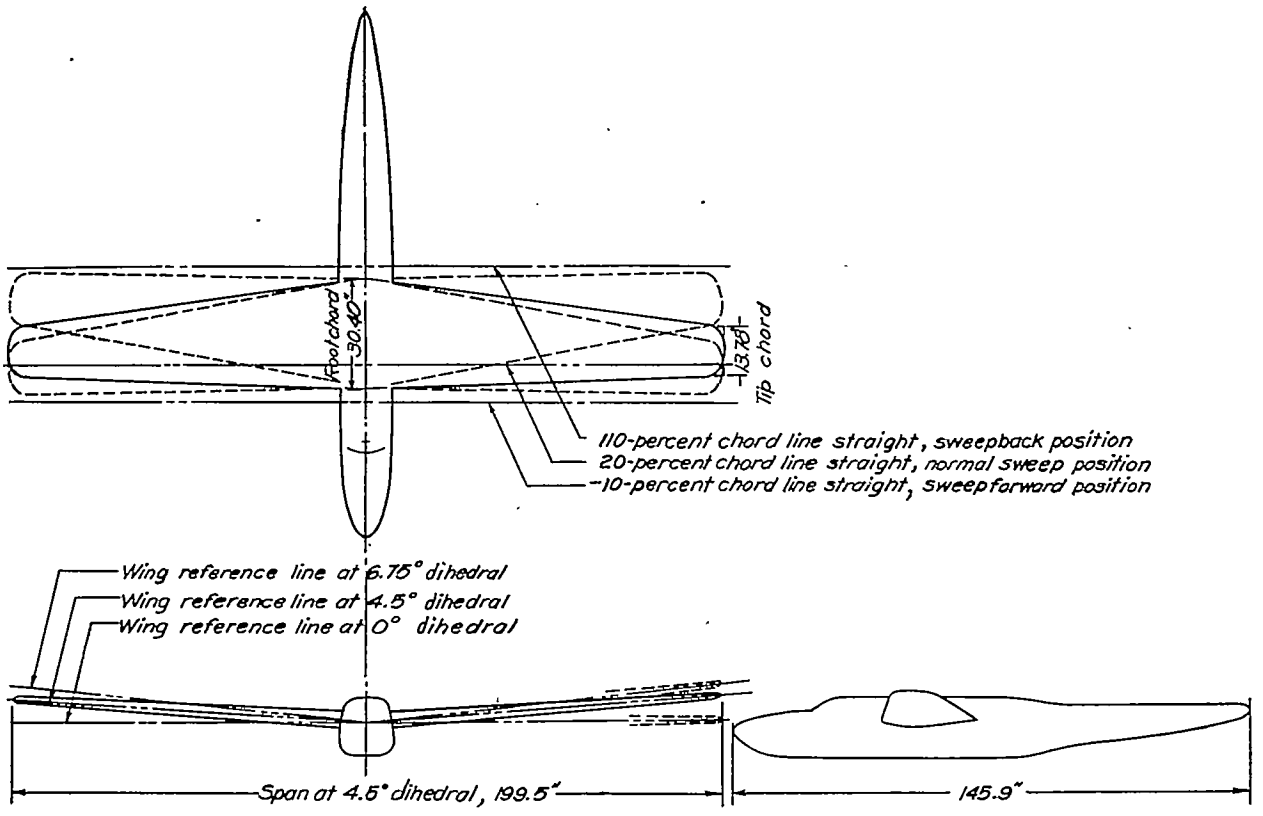

FIGURE 1.—Wing-fuselage combination.

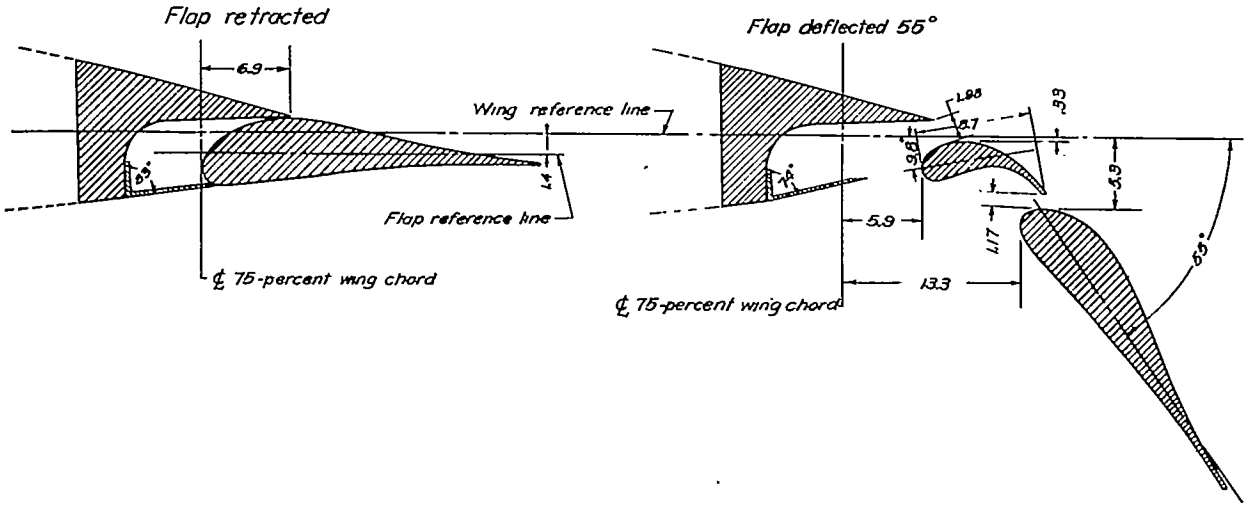

FIGURE 2.—Details of 65-percent-span double slotted flap on wing-fuselage combination. (Dimensions are given in percent wing chord, flaps retracted.)

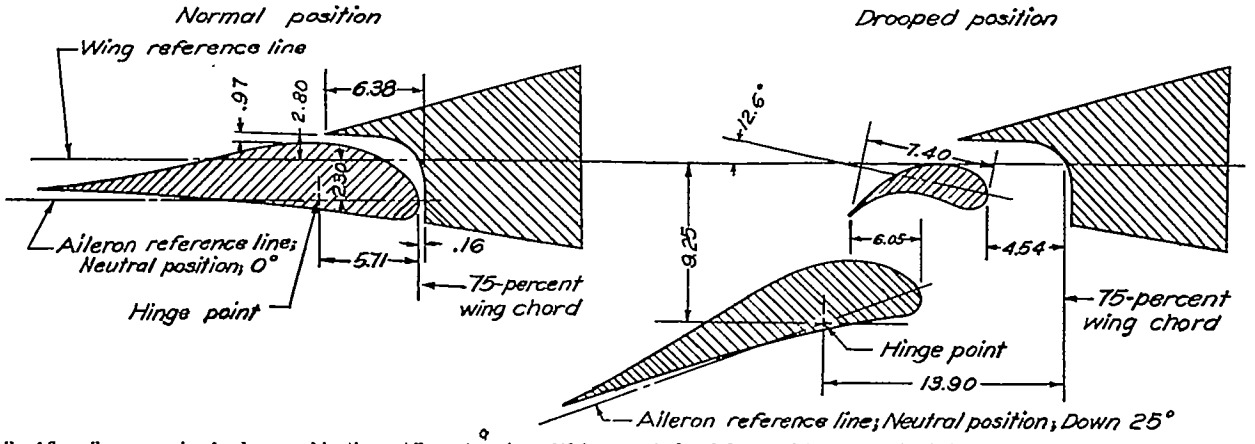

FIGURE 3.—Details of flap-aileron on wing-fuselage combination. Aileron travel, up 20° from neutral and down 15° from neutral. (Dimensions are given in percent of normal wing chord.)

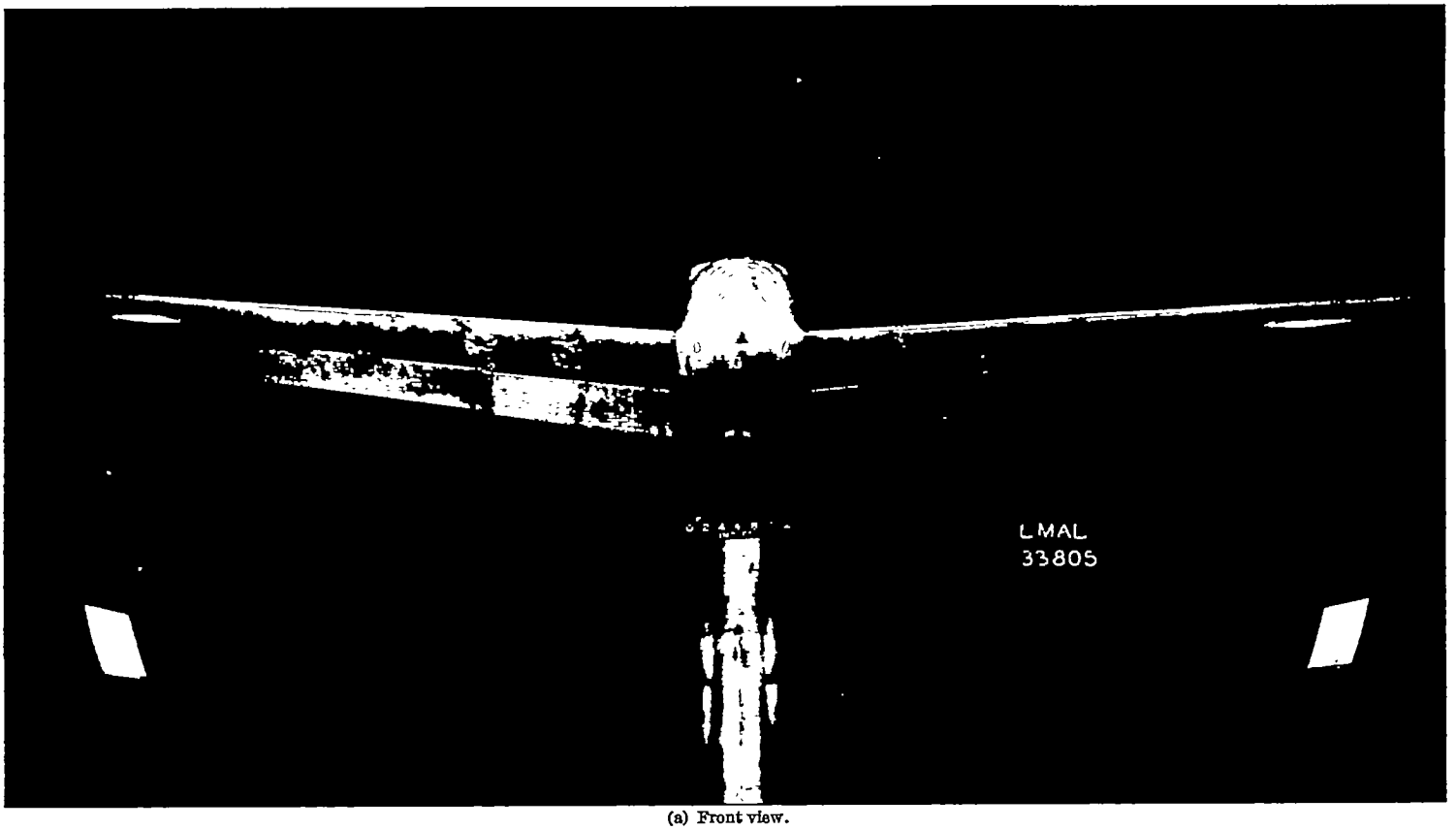

(a) Front view.

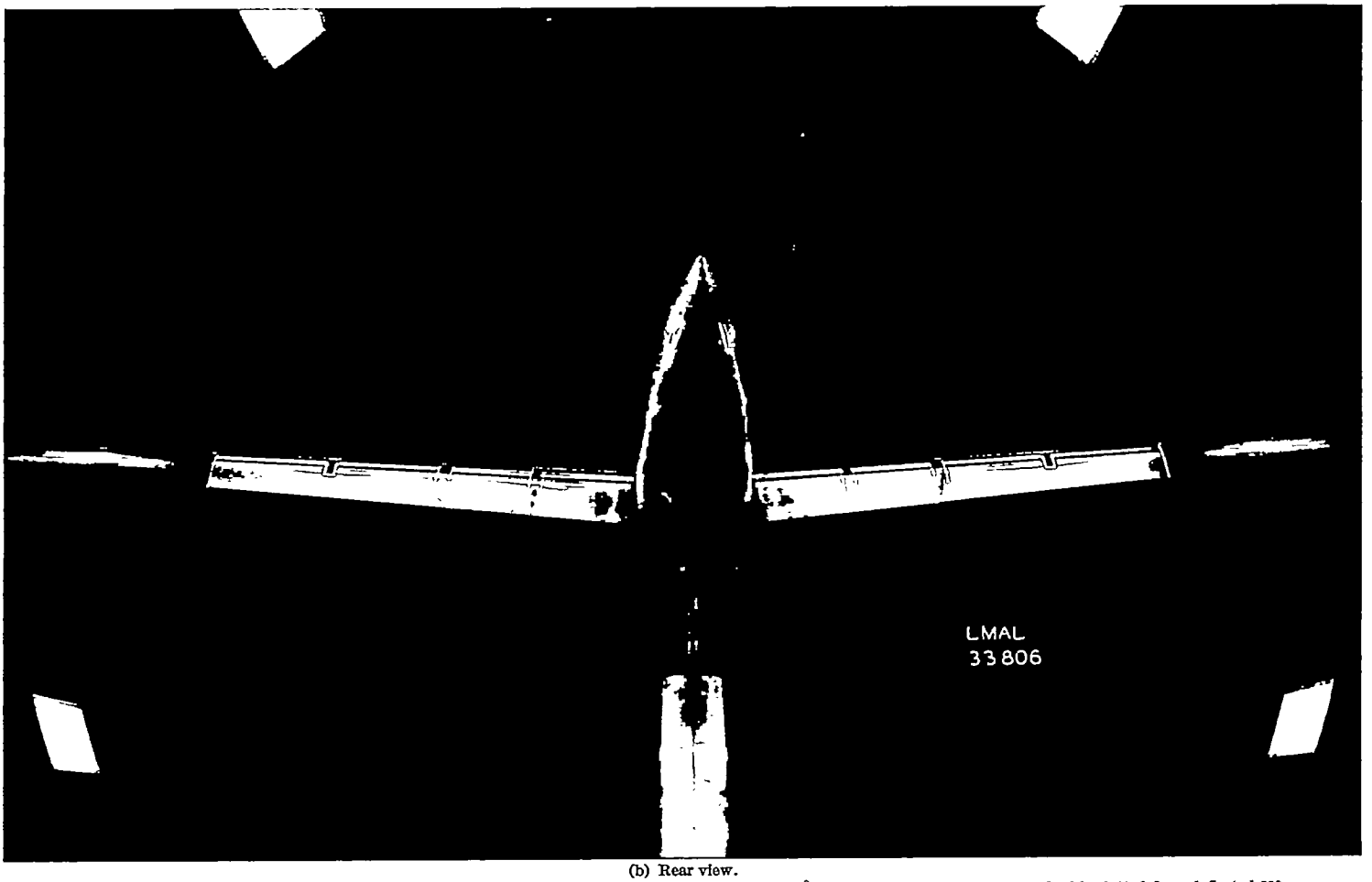

(b) Rear view.

FIGURE 4.—Wing-fuselage combination mounted on single-strut support system in NACA 19-foot pressure tunnel. 65-percent-span double slotted flaps deflected 55°.

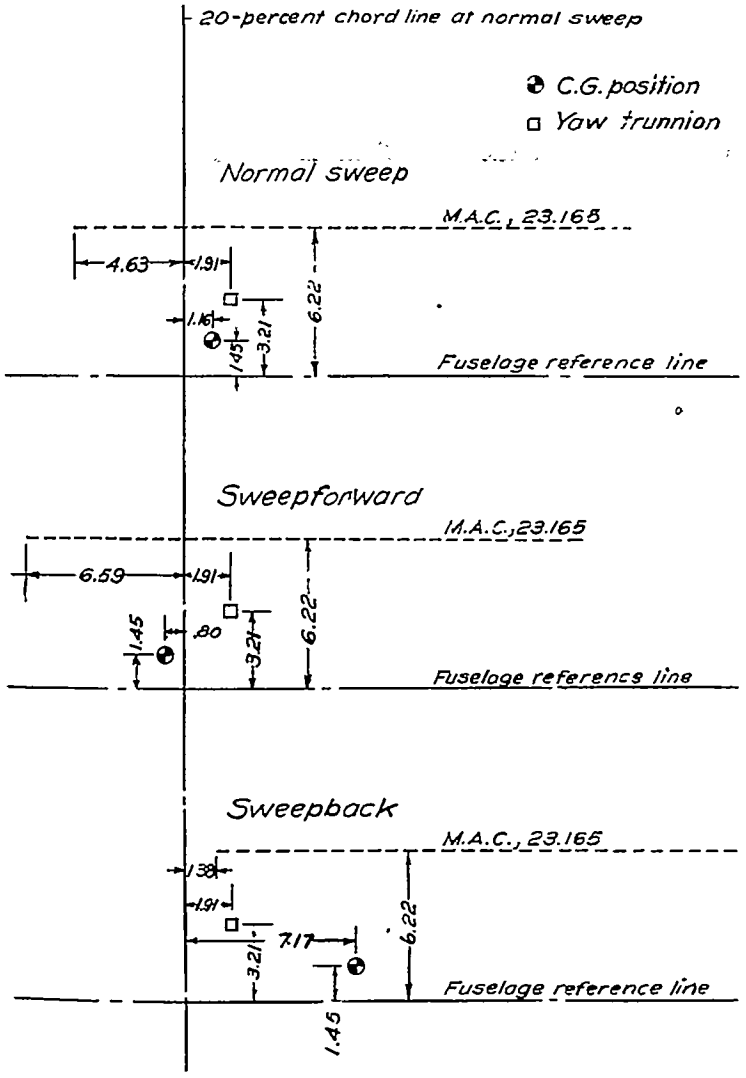

FIGURE 5.—Skeleton-wing diagram showing locations of mean aerodynamic chord, trunnion, and center of gravity. (All dimensions are in inches.)

the fuselage reference line. Figure 5 shows the effect of sweep on the location of the mean aerodynamic chord and corresponding assumed center-of-gravity locations. It should be noted that the vertical location of the center of gravity remained constant with variations in dihedral.

The angle of attack, drag coefficients, and rolling- and yawing-moment coefficients due to deflected ailerons have been corrected for jet-boundary effects. Since all results are essentially comparative, no tare corrections have been applied.

For convenience in locating the results, table I is included.

LONGITUDINAL CHARACTERISTICS

Lift and drag.—The effects of changes in sweep and dihedral on lift and drag are shown in figures 6 and 7, respectively.

For every flap deflection, the greatest angle of stall and the highest value of $C_{L_{max}}$ were noted for the configuration with sweepback. Although this effect differs from that normally expected for sweptback wings, it should be emphasized that the amount of sweepback in the present tests was relatively small. Possibly contributing to the effect of delayed stall in the case of the sweptback wing were decreased inflow and slower progression of stalling. A very slight decrease in the lift-curve slope was measured with sweepback for every flap deflection; whereas, with the full-span flaps deflected, sweepforward showed a slightly higher lift-curve slope than normal sweep. Because the section profiles were altered when the wing sweep was changed, the angle of attack for zero lift was changed with sweep. Sweepback caused the angle of attack for zero lift to be shifted positively. Slightly higher increments of lift coefficient due to partial- and full-span-flap deflection were measured with sweepforward. Sweepback showed a slight reduction in drag coefficient at moderate and high lift coefficients.

Increasing the wing dihedral increased $C_{L_{max}}$ slightly. With partial- and full-span flaps deflected, slightly lower drag was measured with the smallest dihedral.

Pitching moment.—As shown in figure 6, the slopes of the pitching-moment-coefficient curves are practically unaffected by small angles of sweep. These pitching-moment coefficients were computed about center-of-gravity locations 25 percent of the mean aerodynamic chord behind the leading edge of the mean aerodynamic chord and at a fixed location above the fuselage reference line. It should be noted that the introduction of sweep on a particular airplane might have a beneficial effect on the static longitudinal stability because of an effective rearward shift of the aerodynamic center with respect to the center of gravity.

Stall.—Stalling characteristics generally became less desirable as the wing was swept back. The effect of sweep on the stalling characteristics as shown by the tuft behavior is presented in figures 8 to 10. The effect of sweep with flaps neutral is shown in figure 8. It is seen that the point of initial stall moved outboard with sweepback. In the configuration with sweepforward, stalling started at the wing-fuselage juncture and moved outboard; in the configuration with normal sweep, stalling started at approximately 50 percent of the semispan whereas, with sweepback, stalling started at 60 to 85 percent of the semispan and spread inboard and outboard.

Stalling occurred in approximately the same manner when the 65-percent-span flaps were deflected (fig. 9). Strong inflow over and ahead of the ailerons was noted in each sweep configuration.

The effect of sweep on the stalling characteristics with the full-span flaps deflected is shown in figure 10. In the configuration with normal sweep and full-span flaps deflected, a stalled condition extending to 85 percent of the semispan occurred very rapidly. Stalling again started at the wing-fuselage juncture on the configuration with sweepforward and full-span flaps deflected. An almost sudden stall over the outboard 50 percent of the semispan occurred with sweepback.

For the configurations with normal sweep and sweepforward the flaps, which were stalled at low angles of attack, tended to unstall and remain unstalled throughout the high-lift range. Flow behind the flap brackets was always poor; in addition, though the flap breaks were sealed, stalling occurred at the flap junctures.

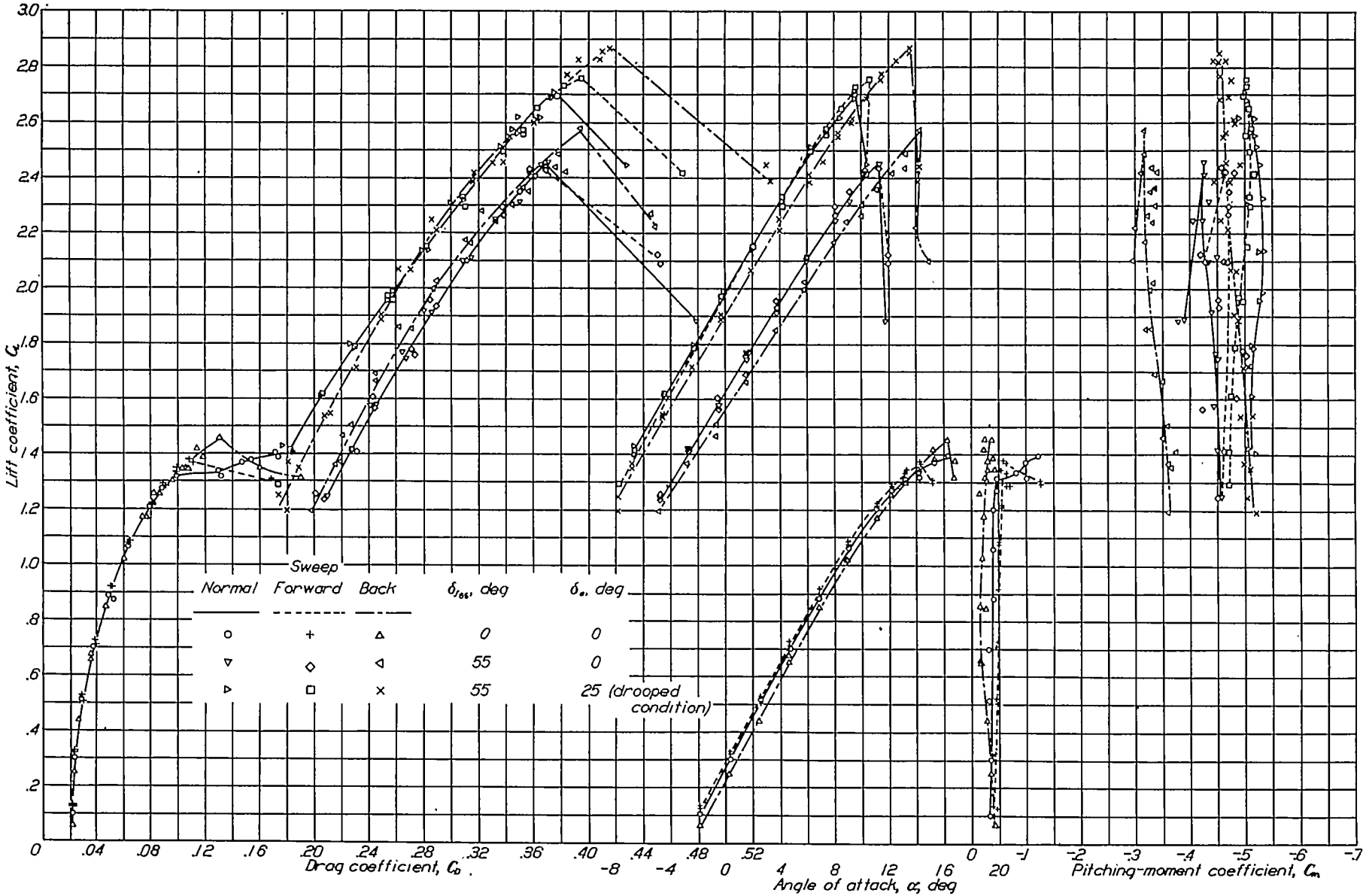

FIGURE 6.—Variation of C_D, α, and C_m with C_L for several sweep and flap configurations. $\Gamma = 4.5°$.

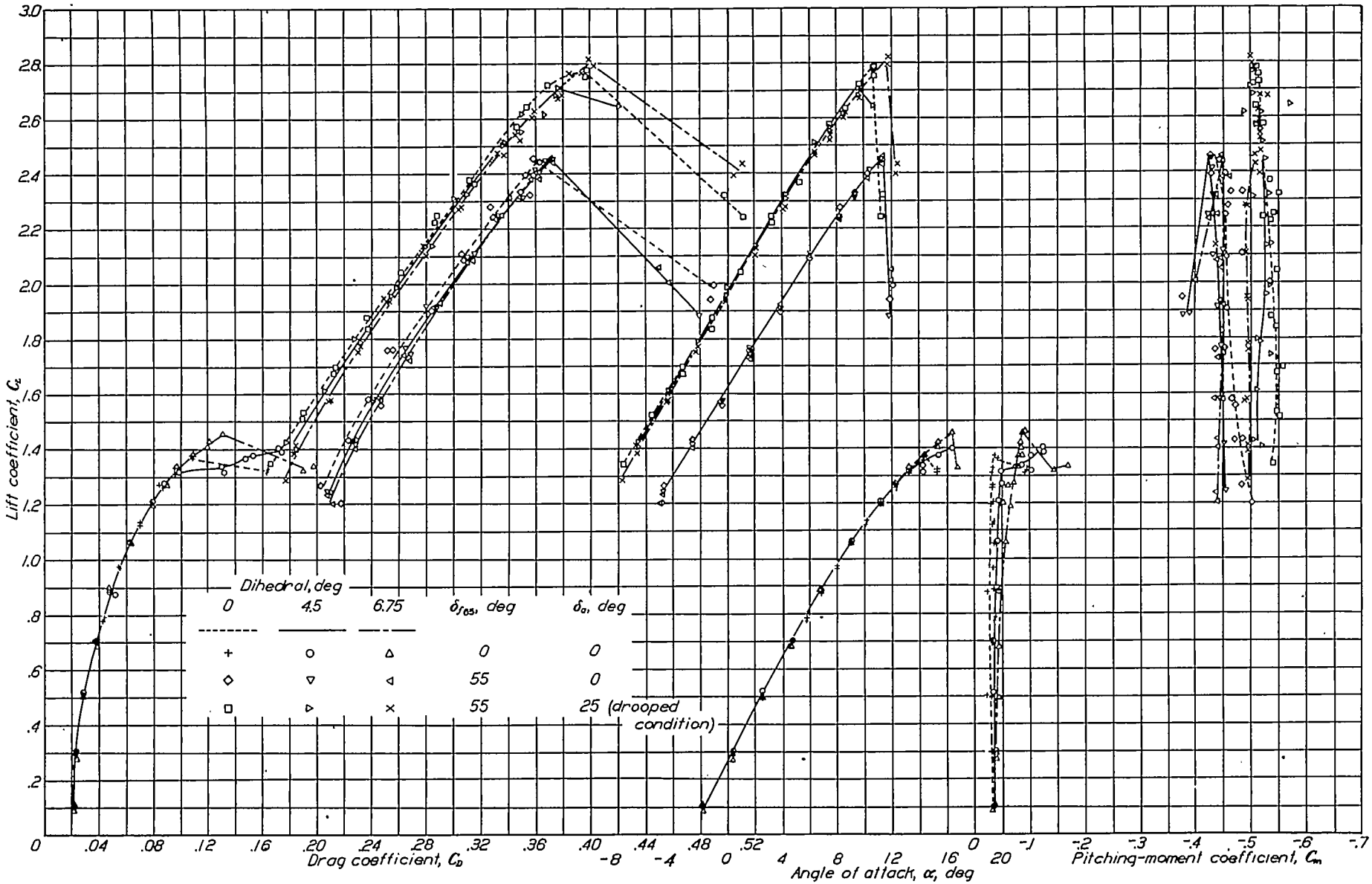

FIGURE 7.—Variation of C_D, α, and C_m with C_L for several dihedral and flap configurations. Normal sweep.

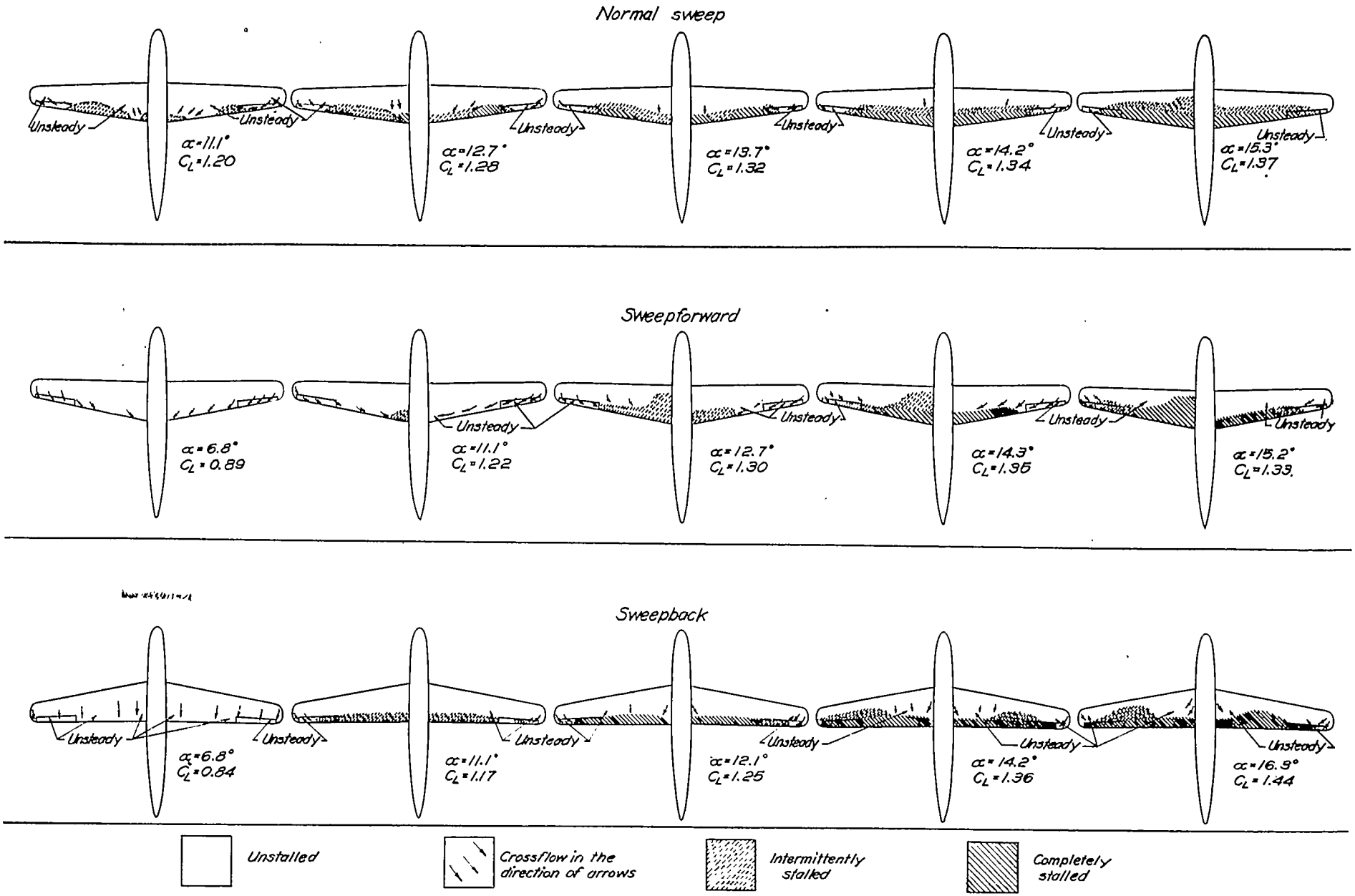

FIGURE 8.—Stall diagrams for several sweep conditions. $\delta_{f_{c/3}}=0°$; $\delta_a=0°$; $\Gamma=4.5°$; $R\approx3.6\times10^6$; $M\approx0.12$.

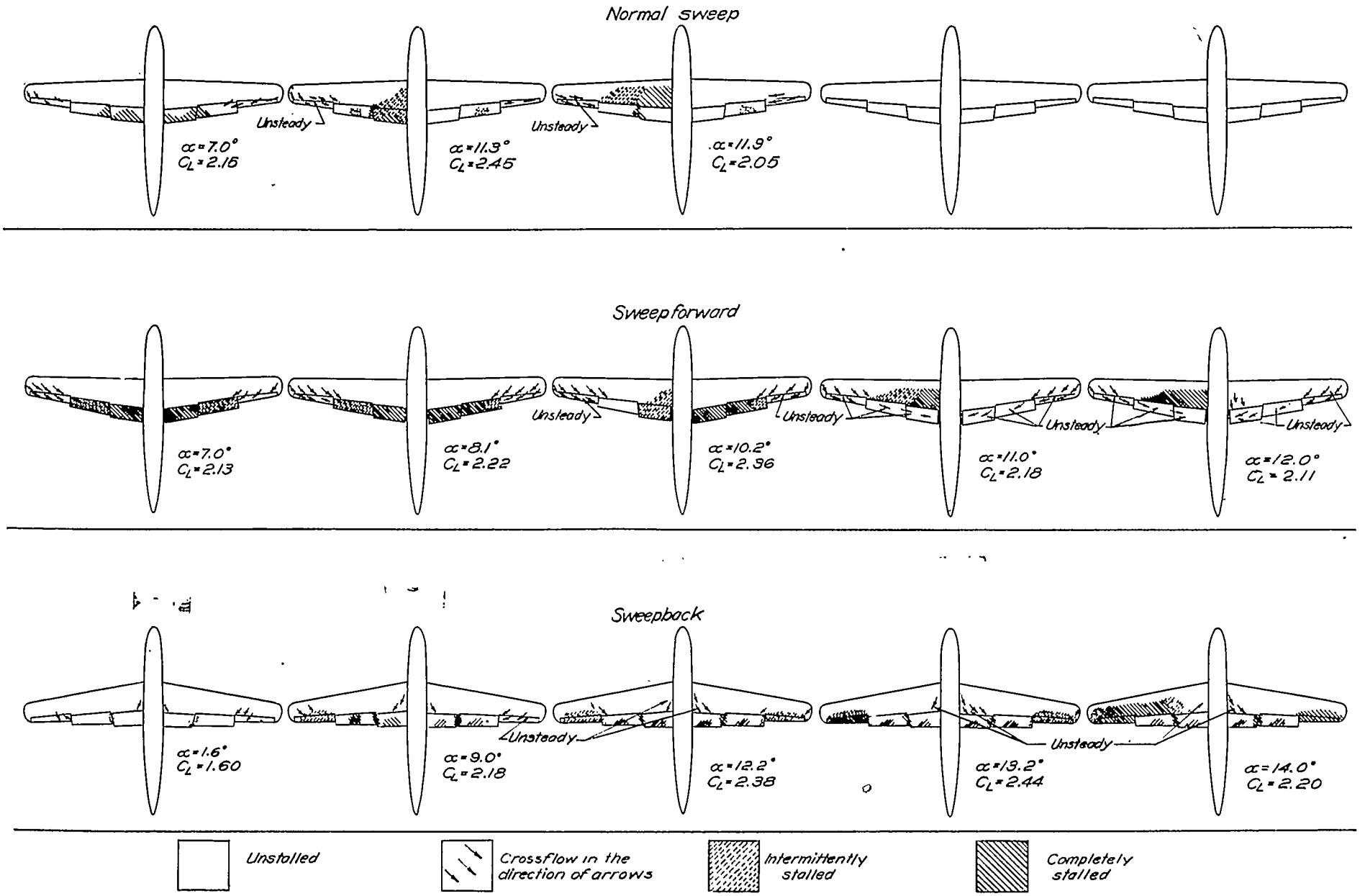

FIGURE 9.—Stall diagrams for several sweep conditions. $\delta_{f_{65}}=65°$; $i_t=0°$; $\Gamma=4.5°$; $R\approx 3.1\times10^6$; $M\approx 0.10$.

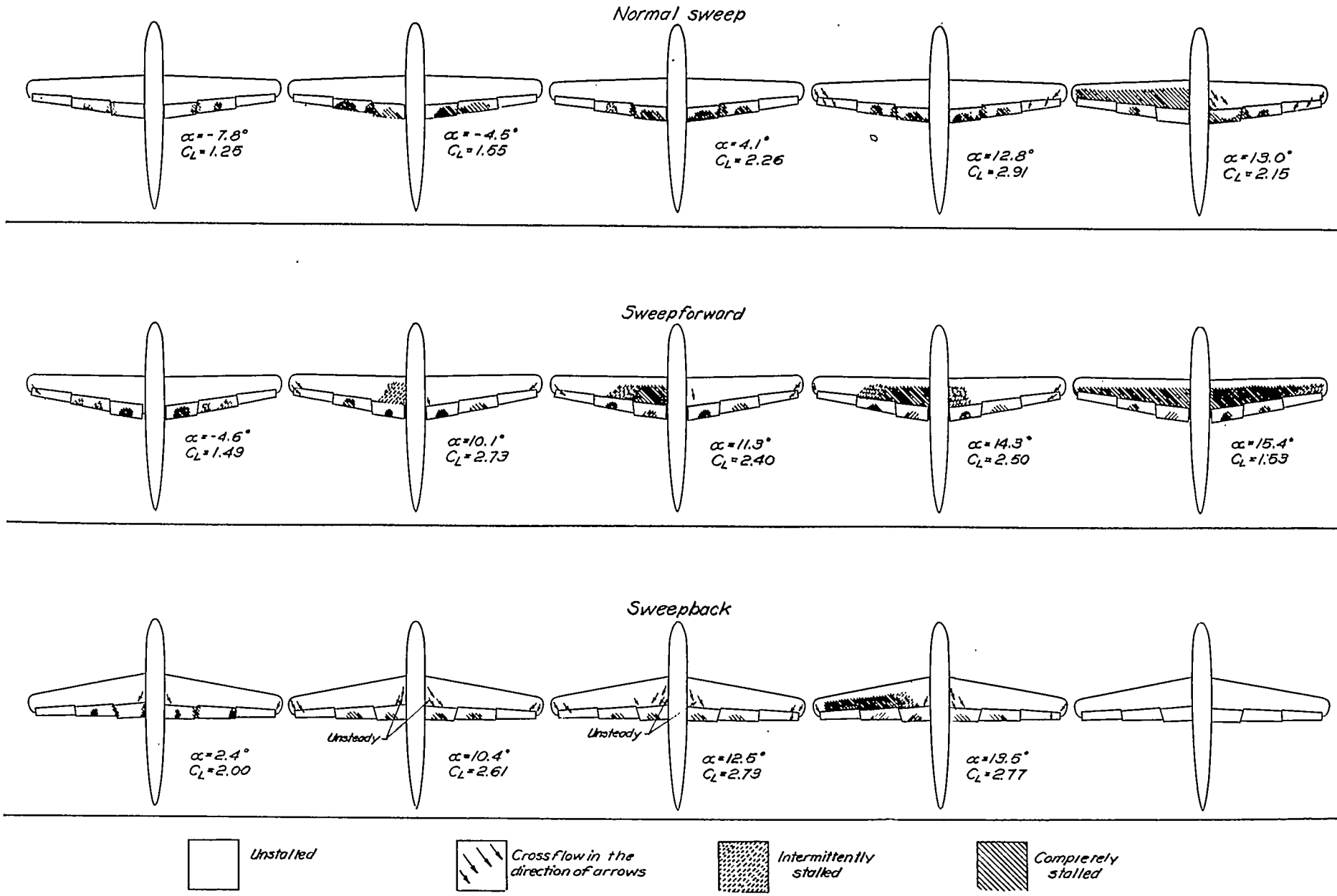

FIGURE 10.—Stall diagrams for several sweep conditions. $\delta_{fu}=55°$; $\delta_a=25°$ (drooped-aileron condition); $\Gamma=4.5°$; $R\approx 2.8\times 10^6$; $M\approx 0.09$.

LATERAL CHARACTERISTICS

The results of the tests to determine the effect of sweep on aileron control are presented in figure 11. Rolling-moment, yawing-moment, and lateral-force coefficients due to aileron deflection have been corrected for model asymmetry. The yaw-test data are presented in figures 12 to 17 and cross plots showing the most significant results are given in figures 18 and 19.

Effect of flap deflection on C_{l_ψ}.—Deflection of the double slotted flaps caused a noticeable reduction in effective dihedral (fig. 19). For the normal-sweep condition, the loss in C_{l_ψ} was approximately 0.00065 or about 2½° effective dihedral and was affected only slightly by a change in flap span. The effect of partial-span split flaps on C_{l_ψ} was found to be negligible (reference 2). It appears, therefore, that the effects of flap deflection on C_{l_ψ} depend upon the type of flap under consideration.

Effect of sweep on aileron effectiveness.—With the flaps neutral, sweepback caused a reduction in aileron effectiveness amounting to approximately 10 percent, whereas a slight increase in aileron effectiveness was noted for the configuration with sweepforward. There was little difference in aileron effectiveness with sweep for the two arrangements with flaps deflected. Little differences in yawing moment due to aileron deflection with sweep were noted. Yawing moment due to aileron deflection was adverse with flaps neutral, became favorable with partial-span flaps deflected, and was more adverse with the full-span flaps deflected.

Effect of geometric dihedral on C_{l_ψ}.—The variation in dihedral effect C_{l_ψ} with dihedral Γ is shown in figure 18. The change in C_{l_ψ} per degree dihedral change averaged approximately 0.00026, which is the value predicted by theory (reference 1).

Effect of sweep on C_{l_ψ}.—As shown in figure 19, sweepback increased the effective dihedral for all flap conditions. The increase in effective dihedral afforded by the change from sweepforward to sweepback varied from less than 2° for flaps retracted and high speed to more than 9° for full-span flaps deflected and low speed.

Sweepback noticeably reduced the loss in effective dihedral caused by deflection of the full-span flaps. The loss due to deflection of the full-span flaps averaged approximately 4°, 2½°, and 1° for sweepforward, normal sweep, and sweepback, respectively. The combination of sweepforward and full-span flaps deflected resulted in an effective dihedral of approximately −1°.

A further advantage of sweepback is shown by the fact that the effective dihedral increases with lift coefficient for all three flap conditions with sweepback. Inasmuch as the adverse effect of power on dihedral effect ordinarily increases with decreasing airspeed, a favorable power-off variation of C_{l_ψ} with C_L as shown by the sweptback wing would be highly desirable. With normal sweep and sweepforward, C_{l_ψ} remained essentially constant over the C_L-range for the two arrangements with flaps deflected; with flaps retracted, however, a less desirable variation existed; that is, C_{l_ψ} decreased with increasing lift coefficient.

Directional stability.—A consistent increase in the unstable directional-stability slope C_{n_ψ} of the wing-fuselage combination accompanied increasing dihedral. The instability increased with angle of attack. This effect is predicted and explained in reference 1. Because the contribution of the fuselage and the wing-fuselage interference effects were not determined, no correlation can be made between the theoretical and test values of C_{n_ψ} as affected by dihedral.

The effect of sweep on C_{n_ψ} was small and irregular. Flap deflection generally caused C_{n_ψ} to increase, though the effect was small.

Lateral force.—C_{Y_ψ} was found to increase slightly with dihedral and angle of attack; flap deflection, however, almost completely erased the effect. Sweep apparently had no effect on C_{Y_ψ}.

CONCLUSIONS

Wind-tunnel tests of a wing-fuselage combination incorporating NACA 65-series airfoil sections were made to determine the effects of small angles of sweep and moderate amounts of dihedral on stalling and lateral characteristics. The following conclusions may be drawn from the results of these tests:

1. Sweepback caused an appreciable increase in positive dihedral effect; sweepforward caused a reduction.
2. The increase in dihedral effect caused by sweepback varied favorably with air speed, in that it increased with lift coefficient.
3. Deflection of double slotted flaps resulted in a noticeable reduction in effective dihedral; sweepback decreased and sweepforward increased this effect.
4. Sweepback moved the point of initial stall outboard and caused a slight increase in maximum lift coefficient.
5. Sweepback caused a reduction in aileron effectiveness of approximately 10 percent with flaps neutral. With partial- or full-span flaps deflected, sweep caused no noticeable change in aileron effectiveness.
6. Standard theoretical methods for predicting the effects of dihedral changes on lateral- and directional-stability derivatives appear valid and unaffected by changes in wing section. For the wing plan form used in the present tests, an increase in the lateral-stability derivative C_{l_ψ} of 0.00026 per degree change in geometric dihedral angle was noted. Increasing dihedral increased the directional instability of the wing-fuselage combination.
7. The effects of dihedral on the remaining aerodynamic characteristics appeared to be unimportant. The present tests indicated a slight increase in the value of maximum lift coefficient with increasing dihedral. Increasing dihedral also caused a slight increase in the value of the lateral-force derivative C_{Y_ψ} with flaps retracted; little effect was noted with flaps deflected.

LANGLEY MEMORIAL AERONAUTICAL LABORATORY,
NATIONAL ADVISORY COMMITTEE FOR AERONAUTICS,
LANGLEY FIELD, VA., *April 15, 1944.*

REFERENCE

1. Pearson, Henry A., and Jones, Robert T.: Theoretical Stability and Control Characteristics of Wings with Various Amounts of Taper and Twist. NACA Rep. No. 635, 1938.
2. Bamber, M. J., and House, R. O.: Wind-Tunnel Investigation of Effect of Yaw on Lateral-Stability Characteristics. I—Four N. A. C. A. 23012 Wings of Various Plan Forms with and without Dihedral. NACA TN No. 703, 1939.

843110—50——31

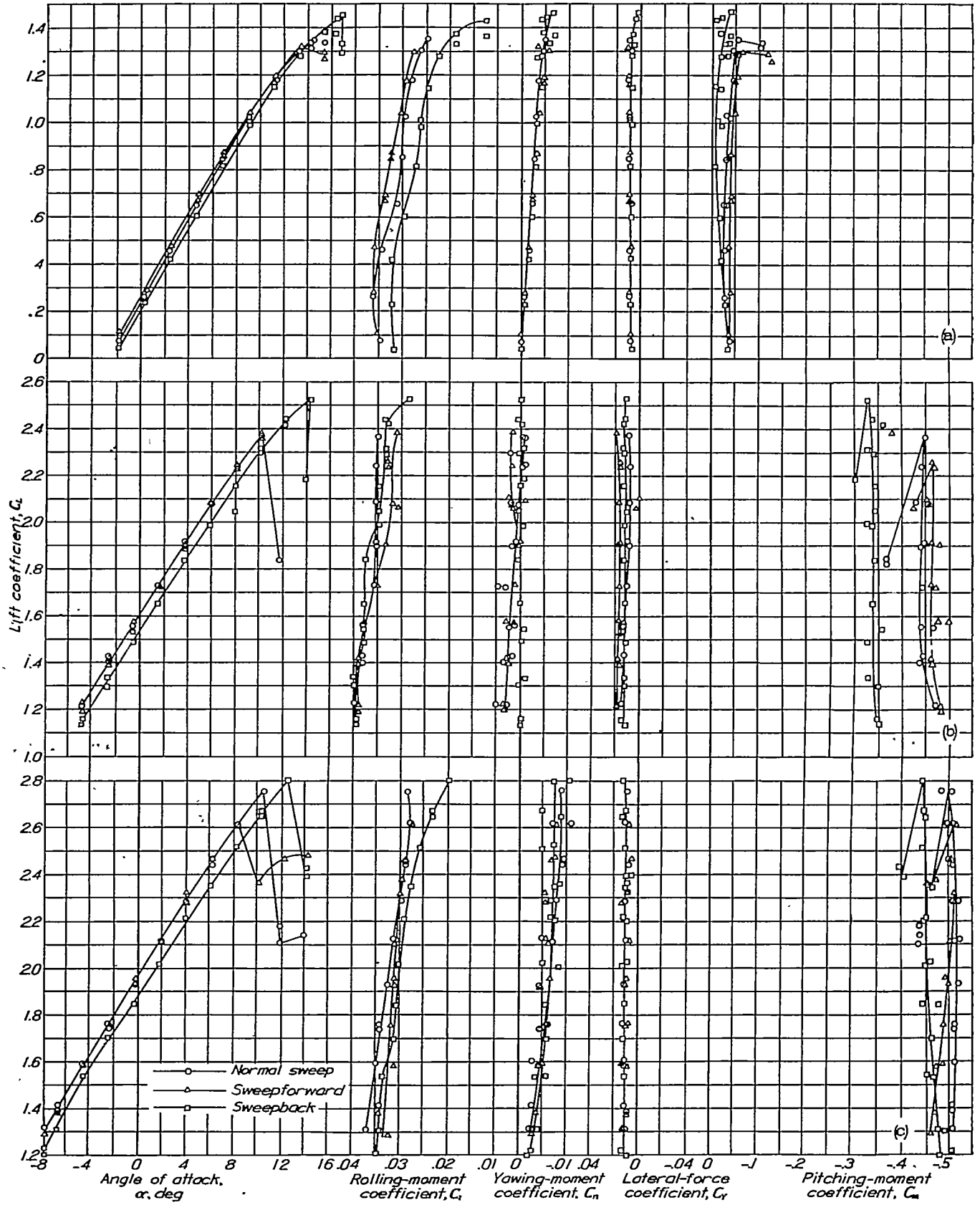

(a) $\delta_{f_{65}}=0°$; $\delta_{a_r}=-12°$; $\delta_{a_l}=9.3°$; $R\approx 3.6\times10^6$; $M\approx 0.12$.

(b) $\delta_{f_{65}}=55°$; $\delta_{a_r}=-12°$; $\delta_{a_l}=9.3°$; $R\approx 3.1\times10^6$; $M\approx 0.10$.

(c) $\delta_{f_{65}}=55°$; $\delta_{a_r}=13°$; $\delta_{a_l}=34.3°$; $R\approx 2.8\times10^6$; $M\approx 0.09$.

FIGURE 11.—Effect of sweep on aileron control. $\Gamma=4.5°$.

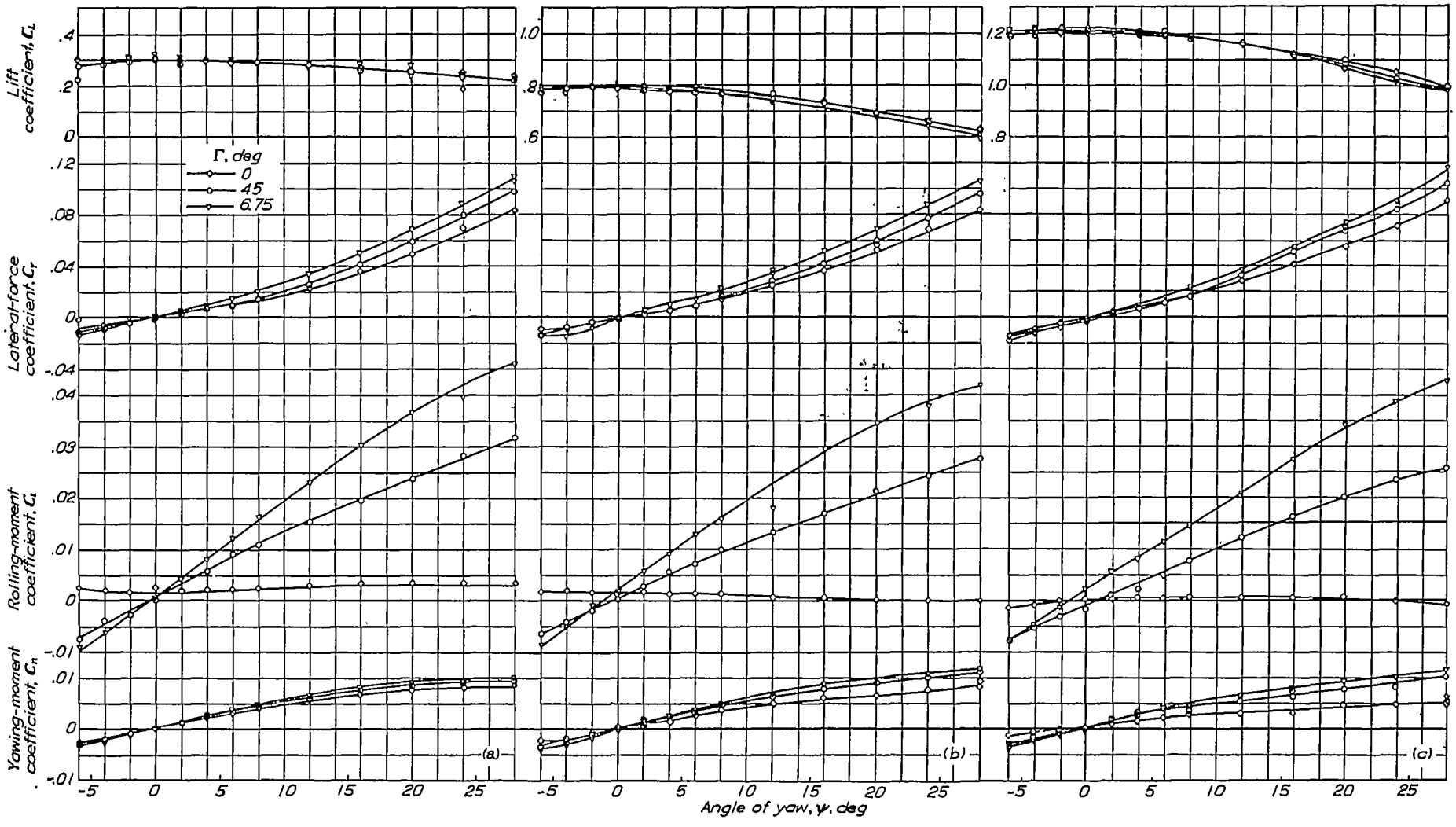

(a) α=0.3°. (b) α=5.7°. (c) α=11.1°.

FIGURE 12.—Variation of C_n, C_l, C_Y, and C_L with ψ for three dihedral conditions. $\delta_{f_{65}}$=0°; δ_{a_r}=δ_{a_l}=0°; normal sweep; $R\approx 3.6\times10^6$; $M\approx$0.12.

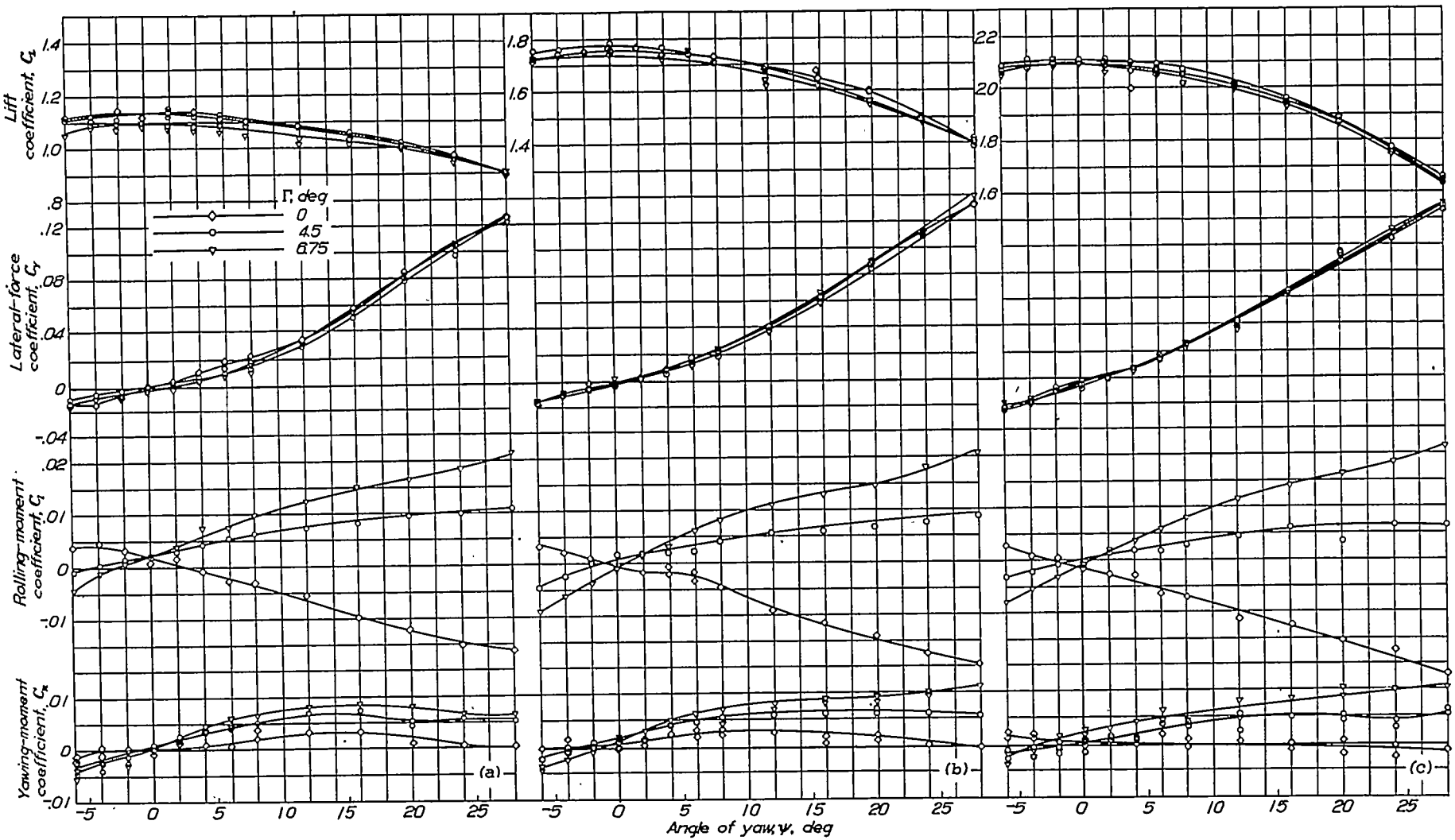

(a) $\alpha = -6.0°$. (b) $\alpha = 1.7°$. (c) $\alpha = 6.0°$.

FIGURE 13.—Variation of C_n, C_l, C_Y, and C_L with ψ for three dihedral conditions. $\delta_{l_3} = 55°$; $\delta_{a_r} = \delta_{a_l} = 0°$; normal sweep; $R \approx 3.1 \times 10^6$; $M \approx 0.10$.

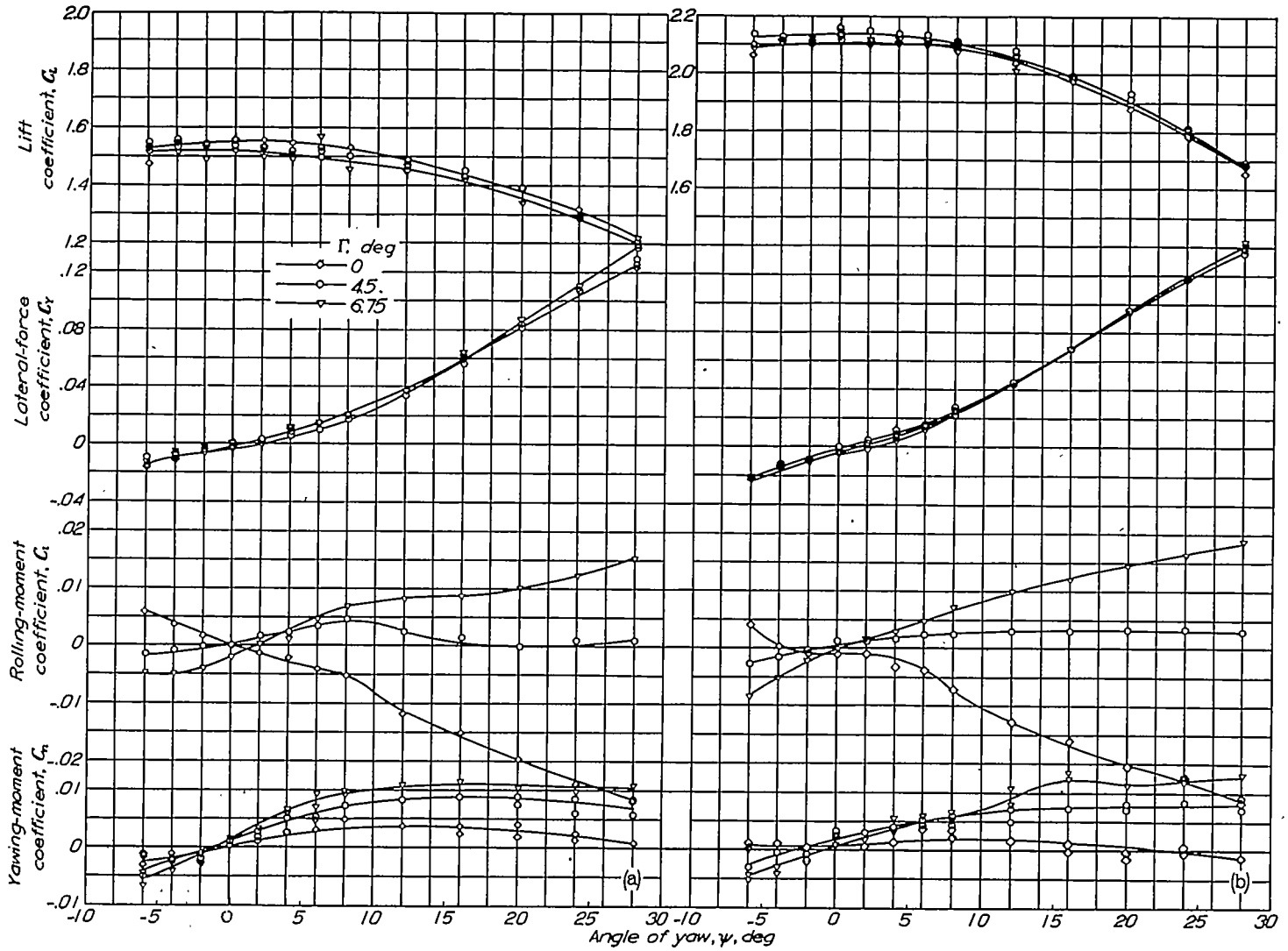

(a) $\alpha = -5.4°$. (b) $\alpha = 2.0°$.

FIGURE 14.—Variation of C_n, C_l, C_Y, and C_L with ψ for three dihedral conditions. $\delta_{f_3} = 55°$; $\delta_{a_r} = \delta_{a_l} = 25°$; normal sweep; $R \approx 2.8 \times 10^6$; $M \approx 0.09$.

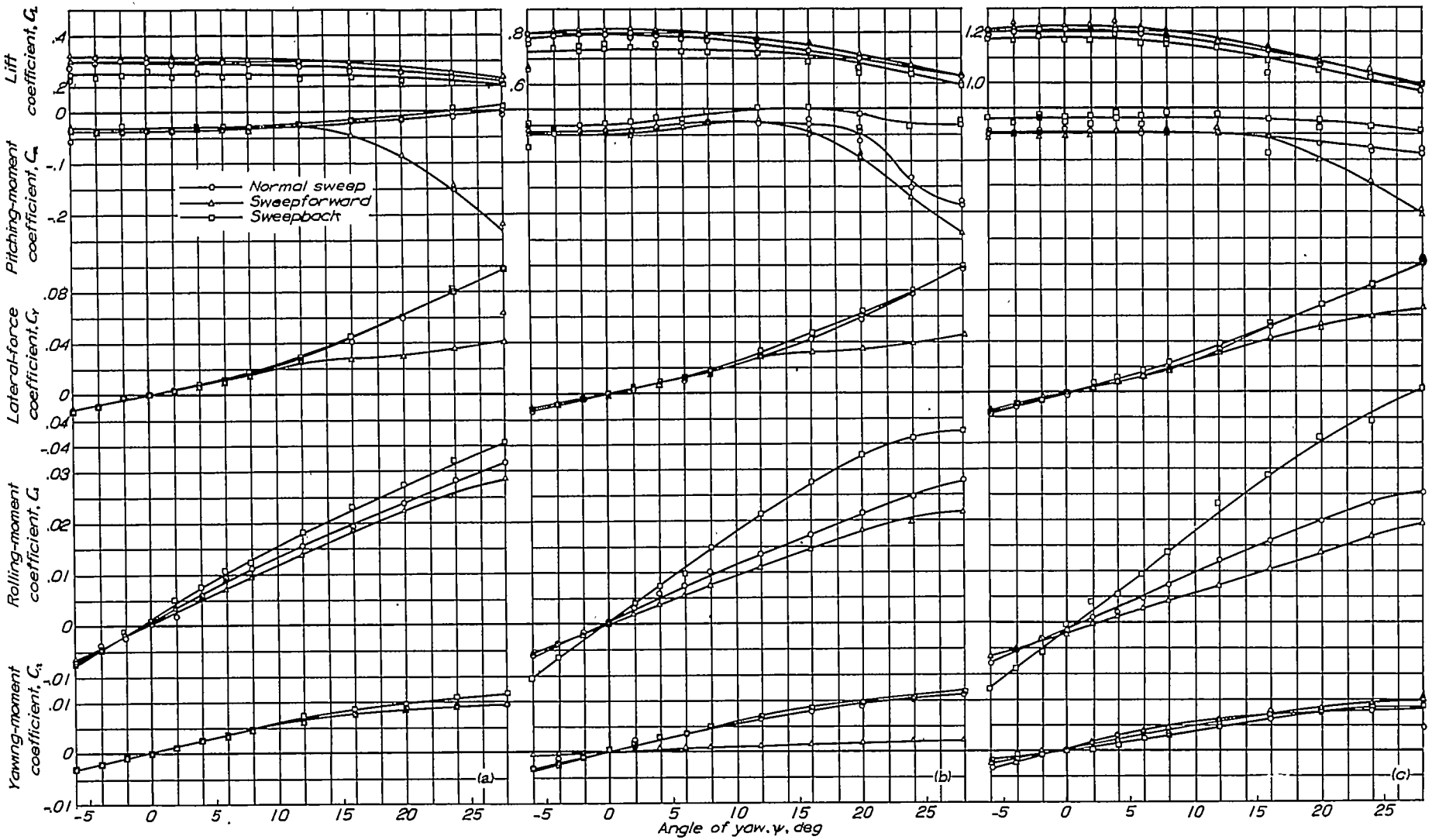

(a) α=0.3°. (b) α=5.7°. (c) α=11.1°.

FIGURE 15.—Variation of C_n, C_l, C_Y, C_m, and C_L with ψ for three sweep conditions. δ_{f_3}=0°; δ_{a_r}=δ_{a_l}=0°; Γ=4.5°; $R\approx 3.6\times 10^6$; $M\approx 0.12$.

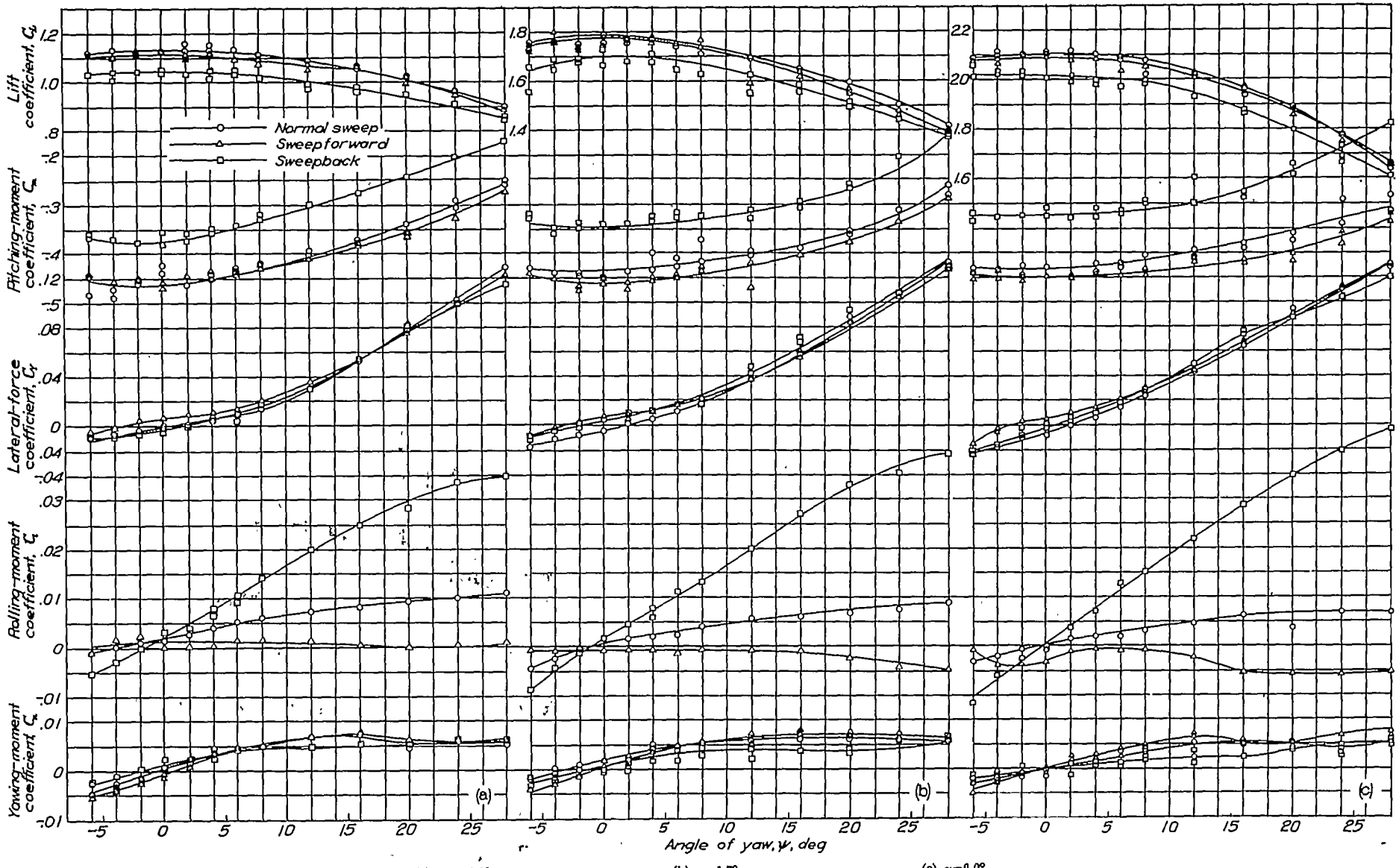

(a) $\alpha \doteq -0.0°$. (b) $\alpha \doteq 1.7°$. (c) $\alpha \doteq 6.0°$.

FIGURE 10.—Variation of C_n, C_l, C_Y, C_m, and C_L with ψ for three sweep conditions; $\delta_{f_{(2)}} = 55°$; $\delta_{a_r} = \delta_{a_l} = 0°$; $\Gamma \approx 4.5°$; $R \approx 3.1 \times 10^6$; $M \approx 0.10$.

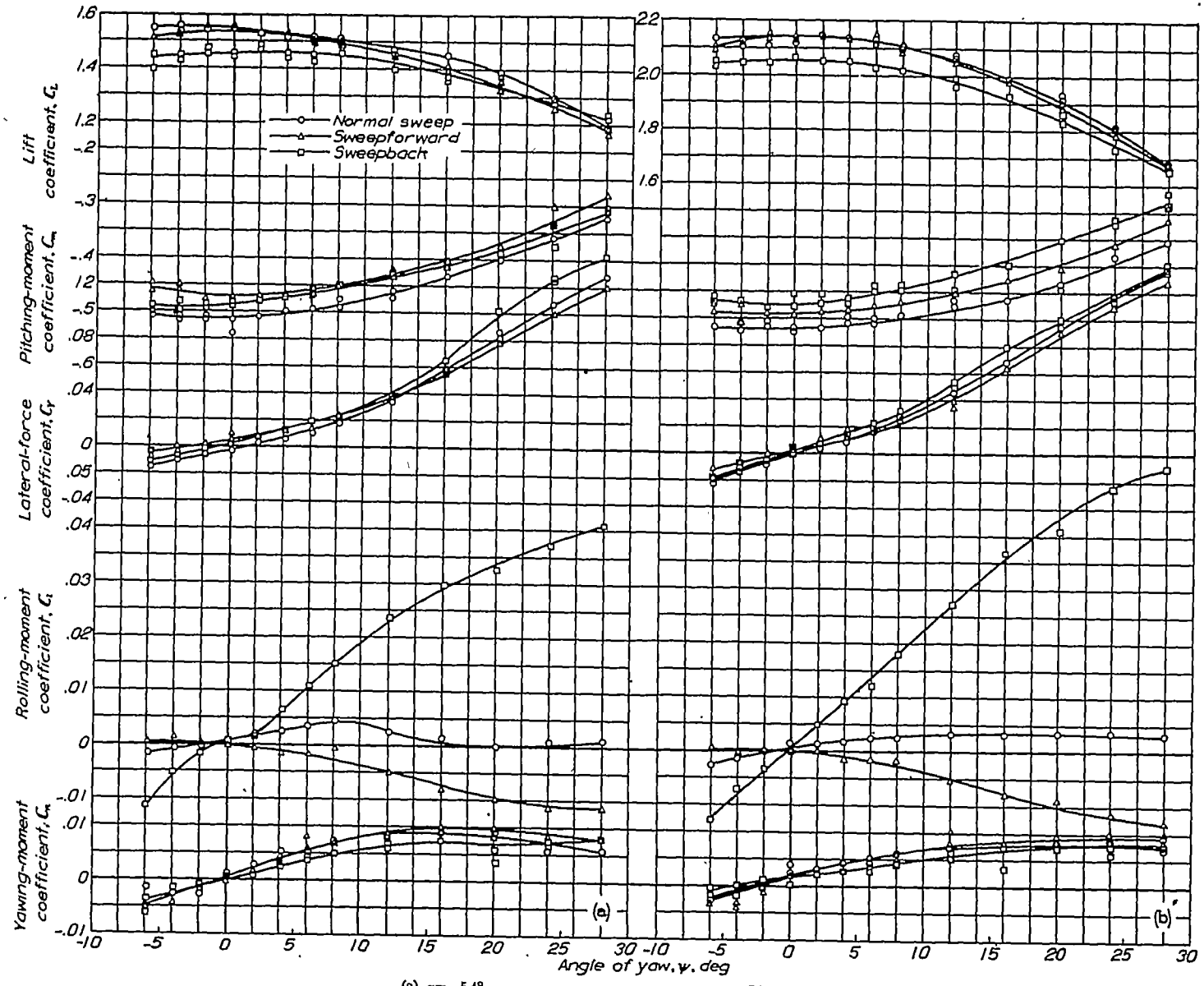

(a) $\alpha = -5.4°$. (b) $\alpha = 2.0°$.

FIGURE 17.—Variation of C_n, C_l, C_Y, C_m, and C_L with ψ for three sweep conditions. $\delta_{f_3} = 55°$; $\delta_{a_r} = \delta_{a_l} = 25°$; $\Gamma = 4.5°$; $R \approx 2.8 \times 10^6$; $M \approx 0.09$.

843110—50——32

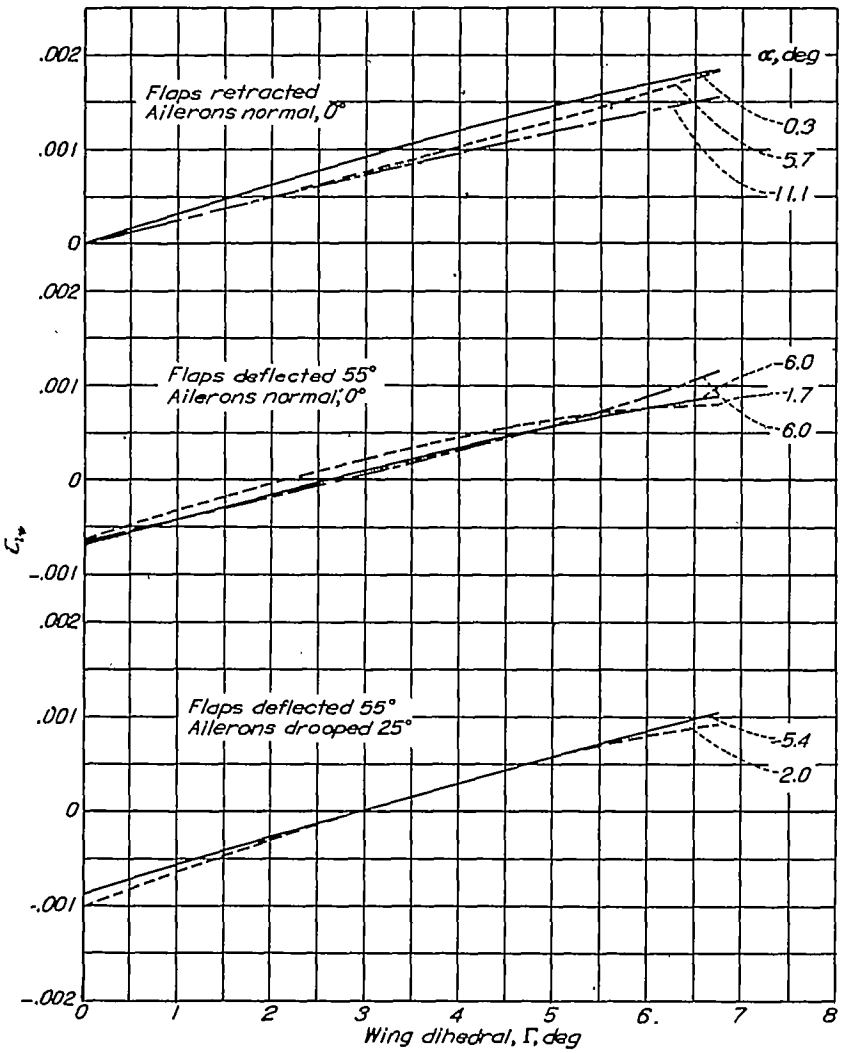

FIGURE 18.—Variation of C_{l_ψ} with Γ for various flap conditions. Normal sweep.

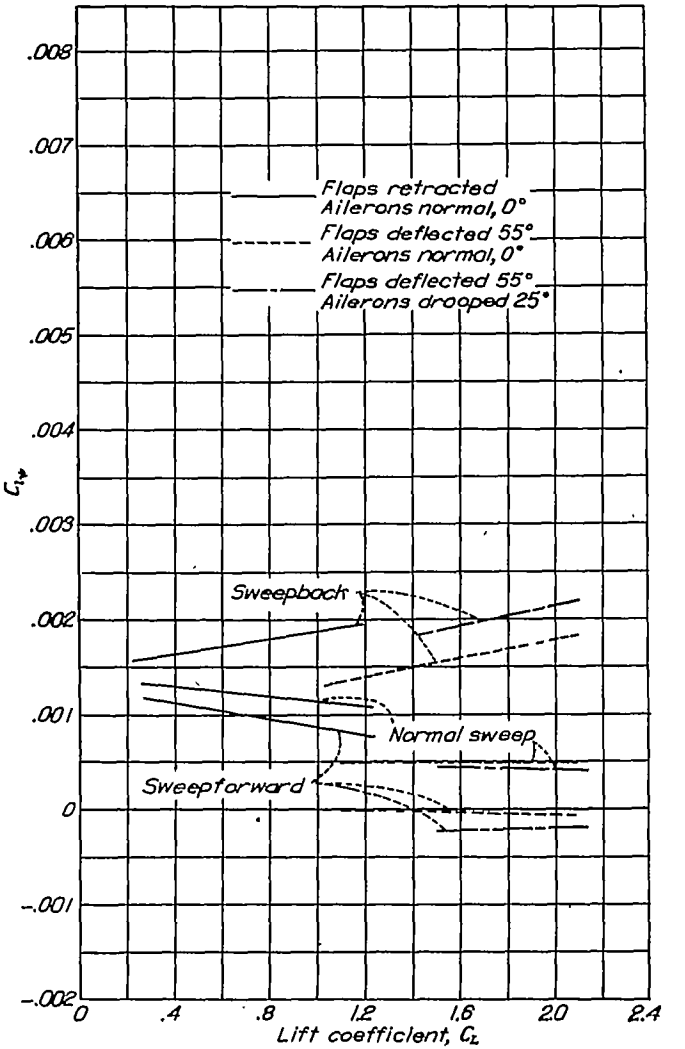

FIGURE 19.—Variation of C_{l_ψ} with C_L for various model configurations. Γ=4.5°.

TABLE I.—PRESENTATION OF DATA

Type of data	Coefficients	Figure	$\delta_{f_{GS}}$ (deg)	δ_{e_r} (deg)	δ_{e_l} (deg)	α (deg)	Γ (deg)	Sweep
Maximum lift	C_D, α, and C_m against C_L	6	0 55 55	0 0 25	0 0 25	Range	4.5	Normal, forward, and back
		7	0 55 55	0 0 25	0 0 25		0, 4.5, and 6.75	Normal
Tuft study		[a] 8	0	0	0	Range	4.5	Normal, forward, and back
		[a] 9	55	0	0			
		[a] 10	55	25	25			
Aileron effectiveness	α, C_l, C_n, C_Y, and C_m against C_L	11(a)	0	−12	9.3	Range	4.5	Normal, forward, and back
		11(b)	55	−12	9.3			
		11(c)	55	13	34.3			
Lateral stability	C_n, C_l, C_Y, and C_L against ψ	12(a)	0	0	0	0.3	0, 4.5, and 6.75	Norma
		12(b)	0	0	0	5.7		
		12(c)	0	0	0	11.1		
		13(a)	55	0	0	−6.0		
		13(b)	55	0	0	1.7		
		13(c)	55	0	0	6.0		
		14(a)	55	25	25	−5.4		
		14(b)	55	25	25	2.0		
Lateral stability	C_n, C_l, C_Y, C_m, and C_L against ψ	15(a)	0	0	0	0.3	4.5	Normal, forward, and back
		15(b)	0	0	0	5.7		
		15(c)	0	0	0	11.1		
		16(a)	55	0	0	−6.0		
		16(b)	55	0	0	1.7		
		16(c)	55	0	0	6.0		
		17(a)	55	25	25	−5.4		
		17(b)	55	25	25	2.0		
Analysis	C_{l_ψ} against Γ	[b] 18	0 55 55	0 0 25	0 0 25	Various	Range	Normal
	C_{l_ψ} against C_L	[c] 19	0 55 55	0 0 25	0 0 25	----------	4.5	Normal, forward, and back

[a] Stall diagrams.
[b] Cross plot of figs. 12 to 14.
[c] Cross plot of figs. 15 to 17.